The equivalent noise bandwidth B_{eq} of a filter is defined by

$$v_{rms}^2 = N_0 B_{eq} \tag{2}$$

where v_{rms} is the output rms voltage with an input of white noise whose power spectral density in V^2/Hz is N_0. The output power v_{rms}^2 is equivalent to that contained in a uniform spectral density N_0 over a hypothetical frequency band of B_{eq} Hz, with zero spectral density elsewhere.

Assuming a filter transfer function $H(s)$, the equivalent bandwidth is given by

$$\begin{aligned} B_{eq} &= \int_0^\infty [H^*(s)H(s)]\,df \\ &= \frac{1}{2}\frac{1}{j2\pi}\int_{-j\infty}^{j\infty} |H(s)|^2\,ds \\ &= \frac{1}{2} I_n. \end{aligned} \tag{3}$$

The squared magnitude of a normalized nth-order low-pass Butterworth filter is

$$|H_n(s)|^2 = \frac{1}{1+\omega^{2n}} \tag{4}$$

where $s=j\omega$. From integral tables [4] the equivalent bandwidth for this case, normalized with respect to the 3-dB bandwidth, is

$$\begin{aligned} \frac{B_{eq}}{B_{3\text{-dB}}} &= \int_0^\infty \frac{d\omega}{1+\omega^{2n}} \\ &= \frac{\pi}{2n\sin\left(\frac{\pi}{2n}\right)}. \end{aligned} \tag{5}$$

The results are listed in Table I as the correct values of equivalent bandwidth. As expected, the equivalent bandwidth approaches the 3-dB bandwidth for higher orders (sharper cutoff).

The transfer function of a normalized nth-order low-pass Butterworth filter is

$$H_n(s) = \frac{1}{s^n + b_{n-1}s^{n-1} + \cdots + b_1 s + 1}. \tag{6a}$$

The coefficients for the denominator polynomials can be calculated from the recursion formula [5]

$$b_{k+1} = \frac{\cos\left(\frac{k}{2n}\right)}{\sin\left(\frac{k+1}{2n}\right)} b_k \tag{6b}$$

starting from $b_0=1$. This polynomial is symmetric: $b_i=b_{n-i}$.

The normalized equivalent bandwidths were calculated from these transfer functions for the first ten orders of Butterworth filters using the formulas from Seifert and Steeg [2], and are listed in Table I. The writer has thoroughly rechecked these calculations and is convinced that they faithfully represent the formulas given in [2].

A very compact derivation of a general formula for I_n has been given by Battin [3]. The numerator polynomial is first multiplied out with its complex conjugate, producing a numerator polynomial of order $2n-2$ in even powers of s (this polynomial often consists of only one nonzero term). Then the integral is of the form

$$I_n = \frac{1}{j2\pi}\int_{-j\infty}^{j\infty} \frac{a_{2n-2}s^{2n-2} + a_{2n-4}s^{2n-4} + \cdots + a_0}{|b_n s^n + b_{n-1}s^{n-1} + \cdots + b_0|^2}\,ds \tag{7a}$$

$$= \frac{(-1)^{n-1}}{2b_n}\frac{|N_n|}{|D_n|} \tag{7b}$$

where $|N_n|$ and $|D_n|$ are $n\times n$ determinants. The elements of $|D_n|$ are

$$d_{ij} = b_{n-2i+j} \tag{7c}$$

where the indices i and j range from 1 to n; d_{ij} is defined to be zero where $2i-j$ is less than 0 or greater than n. The elements of $|N_n|$ are the same except that the first column is replaced by $a_{2n-2}, a_{2n-4}, \cdots, a_0$ for $i=1, 2, \cdots, n$, respectively.

Equation (7b) is written in the form of Cramer's rule for solving n simultaneous linear algebraic equations, where I_n is the value of the unknown for the first column. However, evaluating determinants for $n>3$ implies laborious expansion by minors, which rapidly becomes impractical for higher orders, even by computer. A much more convenient method is the Gauss-Jordan elimination method [6], which is suitable for solving as many as 15 to 20 simultaneous equations where the computation is carried out with eight to ten significant digits. (More sophisticated methods are available for accurate computation of higher orders of simultaneous equations.) A sample Fortran program for the Gauss-Jordan elimination method, reading in the order n and the matrix elements, is given in [6]. An extension of this program was written computing the matrix elements from the polynomials and calculating only the first unknown (the value of I_n). With the transfer functions calculated as before from (6b), the results of this computer program are as given in Table I.

Conclusions

The tabulated results show that the formulas in [2] for orders 6, 7, 8, and 10 give erroneous results for this case. Although the formula for order 9 does give a fairly good result here, it is not nearly as accurate as that from the computer program, and is therefore also somewhat questionable. (Note that these results did not completely test the formulas in [2], since only the constant term was utilized in the numerator of the integrand.)

TABLE I

Calculated Butterworth Equivalent Noise Bandwidth, $B_{eq}/B_{3\text{-dB}}$

n	Correct Value	Seifert and Steeg	Computer Program
1	1.57080	1.57080	1.57080
2	1.11072	1.11072	1.11072
3	1.04720	1.04720	1.04720
4	1.02617	1.02617	1.02617
5	1.01664	1.01664	1.01664
6	1.01152	−0.36757	1.01152
7	1.00844	0.53815	1.00844
8	1.00645	0.46727	1.00645
9	1.00510	1.00405	1.00510
10	1.00412	0.38301	1.00412
11	1.00341		1.00341
12	1.00286		1.00286
13	1.00244		1.00242
14	1.00210		1.00208
15	1.00183		1.00179
.	.		.
.	.		.
.	.		.
20	1.00103		1.00688

While formulas may have the advantage of simplifying operations for optimizing a function, they have the disadvantages of requiring a separate formula for each order and of being increasingly cumbersome with greater chances of transcription mistakes for higher orders (formula number 10 fills two pages). Because of this and the errors in two consecutive sets of published formulas, it seems unlikely that formulas for the higher orders will ever be very useful. A simple computer program with short computation time and valid for any order is clearly a favorable alternative.

Wesley G. Bradford[1]
Data Syst. Div.
Hughes Aircraft Co.
Culver City, Calif. 90230

References

[1] H. M. James, N. B. Nichols, and R. S. Phillips, Eds., *Theory of Servomechanisms*, vol. 25 (MIT Radiation Lab. Ser). New York: McGraw-Hill, 1947, pp. 333–339, 369–370.
[2] W. W. Seifert and C. W. Steeg, Jr., Eds., *Control Systems Engineering*. New York: McGraw-Hill, 1960, pp. 945–955. (This portion was reprinted from a laboratory report by R. C. Booton, Jr., M. V. Mathews, and W. W. Seifert, MIT, 1953.)
[3] J. H. Laning, Jr., and R. H. Battin, *Random Processes in Automatic Control*. New York: McGraw-Hill, 1956, pp. 207–218, 395–397.
[4] H. B. Dwight, *Tables of Integrals and Other Mathematical Data*, 4th ed. New York: Macmillan, 1961, p. 213.
[5] L. Weinberg, *Network Analysis and Synthesis*. New York: McGraw-Hill, 1962, pp. 494–497.
[6] M. L. James, G. M. Smith, and J. C. Wolford, *Analog and Digital Computer Methods in Engineering Analysis*. Scranton, Pa.: International Textbook, 1964, pp. 262–285.

[1] Presently with the Electrical Engineering Department, University of Southern California, Los Angeles, Calif. 90007.

Optimum Waveforms for Sonar Velocity Discrimination

Abstract—Velocity resolvent wide-band sonar waveforms are derived by using the variational calculus together with some properties of the wide-band ambiguity function.

When a wide-band sonar signal $u(t)$ is reflected from a moving point target, its echo has the form [1] $s^{1/2}u[s(t+\tau)]$, where $s=(1+v/c)/(1-v/c)$ is the Doppler scale factor, v is radial target velocity, and c is speed of sound. Multiplication by $s^{1/2}$ is necessary to preserve signal energy, which is normalized to unity.

If correlation processing [2] is used, receiver performance is determined by the function

$$|X_{ua}^{WB}(\tau, s)|^2 = \left|s^{1/2}\int_{-\infty}^{\infty} u(t)u^*[s(t+\tau)]dt\right|^2. \tag{1}$$

Manuscript received March 31, 1971; revised June 1, 1971.

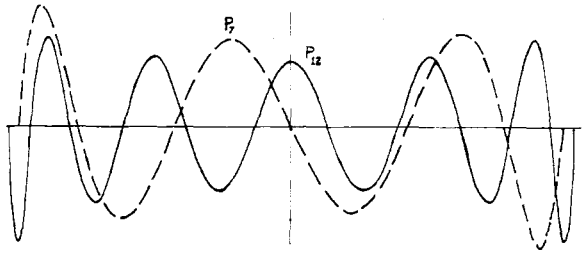

Fig. 1. $P_7(t)$ and $P_{12}(t)$ truncated at their last zero crossings.

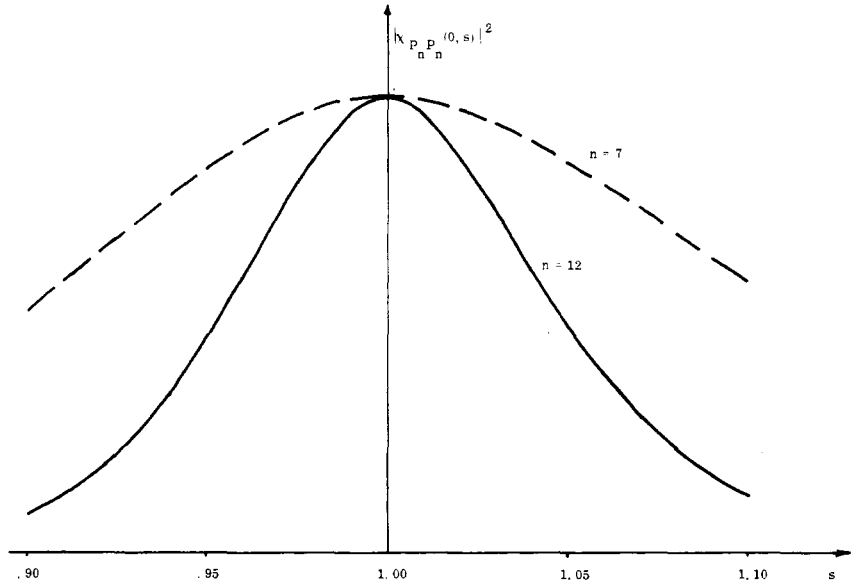

Fig. 2. Doppler axis behavior of $|X_{WB}^{WB}(\tau, s)|^2$, for $u(t) = P_7(t)$ and $P_{12}(t)$, truncated as shown in Fig. 1.

For (τ, s) near (0, 1) [5]

$$\max_{\tau} |X_{WB}^{WB}(\tau, s)|^2 \approx 1 - (\eta^2 - \gamma^2/\lambda^2)(s-1)^2 \quad (2)$$

where [6], if $du(t)/dt = \dot{u}$

$$\eta^2 = \int_{-\infty}^{\infty} t^2|\dot{u}|^2 dt - \left|\int_{-\infty}^{\infty} tu\dot{u}^* dt\right|^2 \quad (3a)$$

$$\lambda^2 = \int_{-\infty}^{\infty} |\dot{u}|^2 dt - \left|\int_{-\infty}^{\infty} u\dot{u}^* dt\right|^2 \quad (3b)$$

$$\gamma = \int_{-\infty}^{\infty} t|\dot{u}|^2 dt - \mathrm{Re}\left\{\int_{-\infty}^{\infty} \dot{u}u^* dt \int_{-\infty}^{\infty} tu\dot{u}^* dt\right\}. \quad (3c)$$

If $u(t)$ is a real function that is either even or odd about $t=0$, then $\gamma = 0$ and

$$\max_{\tau} |X_{WB}^{WB}(\tau, s)|^2 \approx 1 - \eta^2(s-1)^2. \quad (4)$$

An even or odd, real function that maximizes η^2 is thus an optimally Doppler resolvent waveform.

We will make no assumptions about whether the signal is real, even, or odd. We want to find a unit energy signal of the form

$$u(t) = a(t) \exp[j\theta(t)] \quad (5)$$

where $a(t)$ and $\theta(t)$ are such as to maximize η^2. *If* the signal that maximizes η^2 turns out to be real and even or odd, *then* it will follow from (4) that $u(t)$ is an optimally Doppler resolvent waveform.

Physically realizable sonar systems produce waveforms that have finite energy and bandwidth. Energy ($\int|u|^2dt$) and mean square bandwidth ($\int|\dot{u}|^2dt$) are therefore included as constraints, with Lagrange multipliers λ_E and λ_{BW}, respectively. We will also require that

$$u(t) \equiv 0, \qquad \text{for } |t| > 1. \quad (6)$$

Taking the above constraints into account, we wish to maximize the functional

$$\begin{aligned} J(\dot{a}, \dot{\theta}, a) = &\int_{-T}^{T} t^2[\dot{a}^2 + \dot{\theta}^2 a^2]dt \\ &- 1/4\left[\int_{-T}^{T} a^2 dt\right]^2 - \left[\int_{-T}^{T} t\dot{\theta}a^2 dt\right]^2 \\ &- \lambda_{BW}\left[\int_{-T}^{T} (\dot{a}^2 + \dot{\theta}^2 a^2)dt\right] \\ &- \lambda_E \int_{-T}^{T} a^2 dt \\ = &J_1(\dot{a}, a) + J_2(\dot{\theta}, a) \end{aligned} \quad (7)$$

where $0 < T \leq 1$. If $\lambda_{BW} = 1$,

$$J_2(\dot{\theta}, a) = -\int_{-T}^{T} (1 - t^2)\dot{\theta}^2 a^2 dt - \left[\int_{-T}^{T} t\dot{\theta}a^2 dt\right]^2 \quad (8)$$

$J_2(\dot{\theta}, a) \leq 0$ because $|t| \leq T \leq 1$, so that, regardless of $a(t)$, the maximum value of $J_2(\dot{\theta}, a)$ occurs when

$$\dot{\theta}(t) = 0; \qquad \theta(t) = \text{constant}. \quad (9)$$

It remains to maximize the functional

$$J_1(\dot{a}, a) = -\int_{-T}^{T} [(1 - t^2)\dot{a}^2 + (\lambda_E + 1/4)a^2]dt. \quad (10)$$

Applying the Euler and Legendre necessary conditions [3], $J_1(\dot{a}, a)$ is maximized only if

$$(1 - t^2)\ddot{a} - 2t\dot{a} + [n(n+1)]a = 0 \quad (11)$$

where $n(n+1) = -(\lambda_E + 1/4)$. The solutions [4] of the differential equation (11) are Legendre polynomials,

$$a(t) = P_n(t), \qquad |t| \leq T \leq 1. \quad (12)$$

In order that mean square bandwidth ($\int_{-\infty}^{\infty}|\dot{u}|^2dt$) be finite, $u(t)$ can have no discontinuities. We therefore choose T to correspond with the last zero crossing of $P_n(t)$, as shown in Fig. 1.

Because $\dot{\theta}(t) = 0$ and we are interested in the magnitude of $X_{WB}^{WB}(\tau, s)$, we can set $\theta(t) = 0$ without loss of generality. The signal $u(t)$ is thus real and either even (for n even) or odd (n odd) about $t=0$. The signal that maximizes η^2 is then such as to make $\gamma = 0$ in (3c), so that (4) applies and $P_n(t)$ is an optimally Doppler resolvent waveform. The property $\gamma = 0$ implies that the constant magnitude contours of $|X_{WB}^{WB}(\tau, s)|^2$ near $(\tau, s) = (0, 1)$ are symmetrical with respect to the s axis. For $(\tau, s) \approx (0, 1)$ and $s \neq 1$, the maximum value of $|X_{WB}^{WB}(\tau, s)|^2$ occurs for $\tau = 0$, so that

$$\max |X_{WB}^{WB}(\tau, s)|^2 \approx |X_{WB}^{WB}(0, s)|^2.$$

The behavior of $|X_{WB}^{WB}(0, s)|^2$ for $u(t) = P_7(t)$ and $P_{12}(t)$ is shown in Fig. 2.

Any of the solutions $u(t) = kP_n(t), -T \leq t \leq T$, $n = 2, 3, 4, \cdots$, can have a prespecified energy if the scale factor k is correctly adjusted. For a given energy, however, the mean square bandwidth is quantized and depends upon the integer n. To insure the existence of a solution, it is therefore advisable (and physically meaningful) to use an inequality constraint for bandwidth; $\int_{-\infty}^{\infty}|\dot{u}|^2dt \leq B$. The largest allowable value of n is then chosen.

It is possible to make $P_n(t)$ range resolvent as well as Doppler resolvent by simply compressing the waveform in time [6], i.e., if

$$u(t) \rightarrow X_{WB}^{WB}(\tau, s)$$

then

$$a^{1/2}u(at) \rightarrow X_{WB}^{WB}(a\tau, s), \qquad a > 0. \quad (13)$$

If $P_n(t)$ is compressed in time, n must be de-

creased in order to maintain the same upper bound on bandwidth. For a given maximum bandwidth, velocity resolution (Fig. 2) becomes worse as range resolution becomes better. If systems with greater bandwidth are utilized, then these systems must also be capable of generating the high power that will occur when the constant energy waveform is compressed in time. Applicability of (13) is thus limited by both bandwidth and power constraints.[1]

The Fourier transform of $P_n(t)$ is of the form [9] $k\omega^{-1/2}J_{n+1/2}(\omega)$. The time function $kt^{-1/2}J_p(t)$ describes the amplitude of an optimally Doppler *tolerant* waveform [5], the antithesis of the signal derived here.

The waveforms $P_n(t)$ should be useful for sonar velocity measurements (on a single pulse basis). If the sidelobes of $|X_{uu}(\tau, s)|^2$ are small, then the waveforms should also prove useful for the suppression of unwanted reflections from stationary objects (clutter suppression [10]). Although the problem has been formulated for sonar, the result should be applicable to wideband radar as well.

RICHARD A. ALTES
ESL Inc.
Sunnyvale, Calif. 94086

REFERENCES

[1] E. J. Kelly and R. P. Wishner, "Matched-filter theory for high-velocity, accelerating targets," *IEEE Trans. Mil. Electron.*, vol. MIL-9, Jan. 1965, pp. 56–69.
[2] P. M. Woodward, *Probability and Information Theory with Applications to Radar*, 2nd ed. Oxford, England: Pergamon, 1964.
[3] I. M. Gelfand and S. V. Fomin, *Calculus of Variations*. Englewood Cliffs, N. J.: Prentice-Hall, 1963.
[4] E. Jahnke, F. Emde, and F. Losch, *Tables of Higher Functions*. New York: McGraw-Hill, 1960.
[5] R. A. Altes and E. L. Titlebaum, "Bat signals as optimally Doppler tolerant waveforms," *J. Acoust. Soc. Am.*, vol. 48, 1970, pp. 1014–1020.
[6] R. A. Altes, "Methods of wideband signal design for radar and sonar systems," Ph.D. dissertation, The University of Rochester, Rochester, N. Y., 1971.
[7] C. E. Cook and M. Bernfeld, *Radar Signals*. New York: Academic Press, 1967.
[8] W. M. Siebert, "Studies of Woodward's uncertainty function," *Quart. Progress Rept.*, Mass. Inst. Technol., Cambridge, Mass., April 1958, pp. 90–94.
[9] A. Erdélyi *et al.*, *Tables of Integral Transforms*. New York: McGraw-Hill, 1954.
[10] R. A. Altes, "Suppression of radar clutter and multipath effects for wide-band signals," *IEEE Trans. Inform. Theory* (Corresp.), vol. IT-17, May 1971, pp. 344–345.

[1] Although time compression does not affect velocity resolution of wide-band signals, the narrow-band (Woodward) ambiguity function experiences a "stretch" in the velocity variable; $a^{1/2}u(at) \rightarrow X_{uu}^{NB}(a\tau, \phi/a)$. See [7] and [8].

Broad-Band Passive 90° *RC* Hybrid with Low Component Sensitivity for Use in the Video Range of Frequencies

Abstract—A practical 90° hybrid covering the frequency range from 200 Hz to 2 MHz for single-sideband modulation and demodulation can be constructed using cascaded *RC* lattice networks. A differential phase shift within ±6° of 90° can be maintained using 5 percent components.

Manuscript received March 5, 1971.

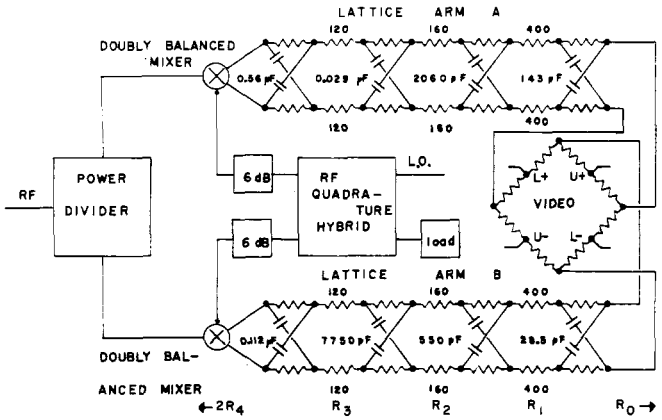

Fig. 1. Circuit of passive SSB modulator–demodulator. All resistances are 2000 Ω unless otherwise noted.

Broad-band 90° phase difference networks operating at video frequencies use *RC* circuits to avoid the use of large inductors. Albersheim and Shirley[1] used *RC* bridge circuits combined with active inverters. Simple *RC* networks of low component sensitivity have been cascaded with active isolation stages by Galpin *et al.*[2] In order to achieve low component sensitivity and avoid active circuits, cascaded *RC* lattice networks have been designed for a "video" hybrid. The elimination of active isolation stages allows the bidirectional use of these networks. The optimum pole-zero pair locations have been computed using the method described by Albersheim and Shirley.[1]

Fig. 1 shows a completely passive SSB modulator–demodulator. The local oscillator signal is divided into quadrature components by an RF quadrature hybrid. Doubly balanced mixers provide balanced and isolated inputs to the differential phase-shifter lattice arms. The sum and the difference of the quadrature video signals are obtained using a resistive bridge network. The video ports (upper and lower sideband are labelled $U+$, $U-$ and $L+$, $L-$) are balanced but isolated so that one of the video terminals can be grounded. Since the hybrid and mixers are bilateral, SSB signals can be generated or detected. When used as a demodulator, the total loss is about a factor of 10 in voltage (ratio of video output voltage to signal input voltage) and the unwanted sideband rejection is greater than 25 dB (in power) from 200 Hz to 2 MHz as illustrated in the measured performance shown in Fig. 2.

Most of the unwanted sideband results from deviations in differential phase shift from 90° by up to 6° while some results from amplitude imbalance. The network is fairly insensitive to component values. At any frequency the phase shift in one lattice arm is at worst changed by 0.25° for 1-percent change in one component. Owing to the balanced and isolated nature of the lattice arms, a 1-percent change of values in any of the components except those making up the summing bridge produces a gain change of less than 0.02 dB in the worst case. Phase errors are not completely accumulative since at any given frequency two lattice sections at most in each arm have any appreciable phase sensitivity. Measurements on several hybrids using 5-percent components show that accumulative errors degrade the unwanted sideband rejection by about 2 dB on average. Bridge phase-shift networks like those described by Albersheim and Shirley[1] use fewer components but have a higher sensitivity. These authors estimate probable cumulative errors in a 90° phase difference network operating from 25 to 6000 Hz to be ±1° in phase and ±0.15 dB in gain for ±1 percent component tolerances.

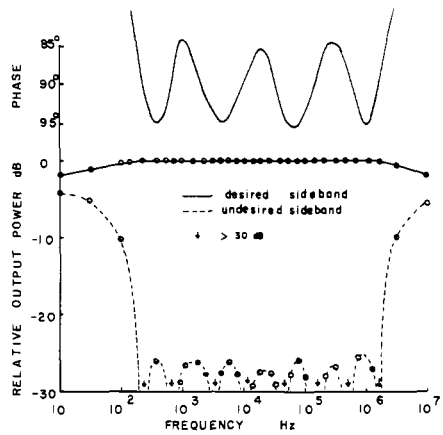

Fig. 2. Relative video output for desired and undesired sidebands. Solid and dashed curves are computed; open circles are measured points. Arrows indicate points where the measured sideband rejection is greater than 30 dB.

The network shown has four zeros in each arm at the locations listed in Table I. The zero locations are simply given by the individual *RC* lattice sections, whereas pole locations are affected by the loading that occurs in the process of cascading lattice networks. The resistive compensation sections are required to move the pole locations to the symmetric locations on the negative real axis required for any all-pass network.

If the compensation conductances are written as $G_0, G_1, G_2, \cdots, G_N$ for the case where *RC* lattice sections all have unit conductance, G_0 is the load conductance (nearest the video

[1] W. J. Albersheim and F. R. Shirley, "Computation methods for broad-band 90° phase-difference network," *IEEE Trans. Circuit Theory*, vol. CT-16, May 1969, pp. 189–196.
[2] R. K. P. Galpin, P. L. Hawkes, W. Saraga, and F. G. Tarbin, "A practical tantalum thin-film single-sideband demodulator using RC time-varying and active networks," *IEEE J. Solid-State Circuits*, vol. SC-2, Mar. 1967, pp. 26–31.